THE JOURNAL OF BIOLOGICAL CHEMISTRY
Vol. 275, No. 17, Issue of April 28, pp. 12781–12788, 2000

Printed in U.S.A.

Calcium Binding to the Photosystem II Subunit CP29*

(Received for publication, November 2, 1999, and in revised form, December 20, 1999)

Caroline Jegerschöld‡§, A. William Rutherford‡, and Tony A. Mattioli‡¶‖

From the ‡Section de Bioénergétique, Département de Biologie Cellulaire et Moléculaire, CEA/Saclay and CNRS URA 2096, 91191 Gif-sur-Yvette cedex, France and the ¶Section de Biophysique des Protéines et des Membranes, Département de Biologie Cellulaire et Moléculaire, CEA/Saclay and CNRS URA 2096, 91191 Gif-sur-Yvette cedex, France

Massimo Crimi and Roberto Bassi****

*From the **Facoltà di Scienze MMFFNN, Biotecnologie Vegetali, Università di Verona, Strada Le Grazie, 37134 Verona, Italy*

We have identified a Ca^{2+}-binding site of the 29-kDa chlorophyll *a/b*-binding protein CP29, a light harvesting protein of photosystem II most likely involved in photoregulation. $^{45}Ca^{2+}$ binding studies and dot blot analyses of CP29 demonstrate that CP29 is a Ca^{2+}-binding protein. The primary sequence of CP29 does not exhibit an obvious Ca^{2+}-binding site therefore we have used Yb^{3+} replacement to analyze this site. Near-infrared Yb^{3+} vibronic side band fluorescence spectroscopy (Roselli, C., Boussac, A., and Mattioli, T. A. (1994) *Proc. Natl. Acad. Sci. U. S. A.* 91, 12897–12901) of Yb^{3+}-reconstituted CP29 indicated a single population of Yb^{3+}-binding sites rich in carboxylic acids, characteristic of Ca^{2+}-binding sites. A structural model of CP29 presents two purported extra-membranar loops which are relatively rich in carboxylic acids, one on the stromae side and one on the lumenal side. The loop on the lumenal side is adjacent to glutamic acid 166 in helix C of CP29, which is known to be the binding site for dicyclohexylcarbodiimide (Pesaresi, P., Sandonà, D., Giuffra, E., and Bassi, R. (1997) *FEBS Lett.* 402, 151–156). Dicyclohexylcarbodiimide binding prevented Ca^{2+} binding, therefore we propose that the Ca^{2+} in CP29 is bound in the domain including the lumenal loop between helices B and C.

Photosystem II (PSII)[1] of cyanobacteria and higher plants is a multisubunit, membrane-spanning enzymatic complex responsible for oxygen evolution resulting from water oxidation. The oxidation of water occurs at the lumenal surface of the thylakoid membrane through the stepwise oxidation of a manganese cluster, $(Mn)_4$, which forms the catalytic core of the oxygen evolving enzyme (see reviews, see Refs. 1–3). PSII water oxidation requires both calcium and chloride ions, and although the calcium requirement has been intensively studied, insight regarding the number of Ca^{2+} sites and the precise role of Ca^{2+} in the photosynthetic oxidation of water remains murky (for review, see Refs. 1–4). It is known that the absence of Ca^{2+} in PSII inhibits proper photochemical function preventing oxygen evolution, and it is now becoming clear that one Ca^{2+}-binding site is associated with these calcium-depleted effects (1–3, 5–8). The marked effects which the removal of Ca^{2+} has on the functioning of the oxygen evolving enzyme strongly suggest that this Ca^{2+} site is located in the reaction center core of PSII (5). Site-directed mutagenesis studies have allowed suggestions concerning the location of the Ca^{2+}-binding site in the PSII reaction center core (9, 10).

Photosystem II possesses a second Ca^{2+}-binding site not directly related to oxygen evolution (5, 11, 12). This second Ca^{2+} ion is very tightly bound and appears to be associated with a light-harvesting protein (5, 12–14). There are conflicting reports as to which of the light-harvesting proteins the strongly bound Ca^{2+} is associated. Irrgang and co-workers (12) have characterized the strong Ca^{2+}-binding properties of a 30-kDa Chl *a/b* protein and reported its implication as being a Ca^{2+}-binding protein. This 30-kDa protein is most likely CP29 (see Ref. 15).

CP29 is the largest of the so-called "minor" light harvesting complex (LHC) proteins of PSII and consists of approximately 257 amino acids. Various data indicate that the protein binds 6 Chl *a*, 2 Chl *b*, and 2 xanthophyll molecules (16–18). CP29 is situated between the major LHCII complex and the PSII core and is thought to play a role in the regulation of the concentration of the Chl *a* excited states (16, 19, 20). CP29 also undergoes reversible phosphorylation under photoinhibitory conditions (21). It seems then that CP29 probably plays important roles in photoregulation in PSII.

In this contribution, we identify a specific Ca^{2+}-binding site in the CP29 polypeptide of maize PSII. CP29 was reconstituted with the lanthanide Yb^{3+} and the metal-binding site in CP29 was characterized using near-infrared Yb^{3+} vibronic side band (VSB) fluorescence spectroscopy (22, 23). In this technique, we exploit the well known phenomenon of the specific replacement of Ca^{2+} in proteins with trivalent lanthanide metal ions (24, 25). After Ca^{2+} is replaced selectively with Yb^{3+}, then the fluorescence spectrum of Yb^{3+} in the Ca^{2+} site is recorded and analyzed. When coordinated, the Yb^{3+} fluorescence spectrum exhibits two characteristic types of features: 1) a sharp 4f-4f electronic feature called the zero phonon line (ZPL) that corresponds to the Yb^{3+} $^2F_{5/2} \rightarrow {}^2F_{7/2}$ electronic transition, and, 2) weak VSBs shifted to longer wavelengths with respect to the ZPL. These VSBs are the result of short-range dipole-dipole interactions that couple the ZPL electronic transition dipole of Yb^{3+} with the dipoles of the vibrational modes of its ligands. These VSBs reflect the vibrational modes of the Yb^{3+} ligands: the spectral energy difference between the ZPL and the various

* This work was supported by a long-term FEBS fellowship (to C. J.) and a grant from "Progetto Finalizzato Biotecnologie" of CNR (to R. B.). The costs of publication of this article were defrayed in part by the payment of page charges. This article must therefore be hereby marked "*advertisement*" in accordance with 18 U.S.C. Section 1734 solely to indicate this fact.

§ Current address: Dept. of Biochemistry, Imperial College of Science, Technology and Medicine, London, SW7 2AY, England.

‖ To whom correspondence should be addressed: Tel.: 33-1-6908-4166; Fax: 33-1-6908-8717; E-mail: mattioli@dsvidf.cea.fr.

[1] The abbreviations used are: PSII, Photosystem II; β-DM, dodecyl-β-maltoside; Chl, chlorophyll; CP, chlorophyll protein; DCCD, dicyclohexylcarbodiimide; MES, 2-[morpholino]ethanesulfonic acid; LHCII, light-harvesting complex II; VSB, vibronic side band; ZPL, zero phonon line.

VSBs correspond to vibrational energies (or frequencies) of the corresponding ligand vibrational modes. VSBs, in fact, provide a specific and selective vibrational spectrum of the ligands and only the ligands defining the binding site of Yb^{3+} in the protein (see Refs. 22 and 23 and references therein). As with Raman or infrared vibrational spectra, Yb^{3+} VSB "fingerprint" spectra can be used to identify the chemical nature of the metal binding ligands. Since inspection of the primary sequence of CP29 (26) does not reveal an obvious Ca^{2+}-binding site such as a classic EF-type motif, the vibrational information obtained from the Yb^{3+} VSB spectra provides valuable information concerning the chemical nature of the binding site of Yb^{3+} reconstituted into the Ca^{2+}-binding site in CP29, and a plausible location may be proposed.

EXPERIMENTAL PROCEDURES

Native CP29 and LHCII were purified from maize PSII membranes as described previously (27, 28). Proteins were transferred to a nitrocellulose membrane (Bio-Rad) with a dot blot apparatus (Bio-Rad) (CP29 = 1.6 μg of Chl; LHCII = 1.7 μg of Chl; calsequestrin = 3.8 μg of protein).

Detection of $^{45}Ca^{2+}$ binding was performed essentially as in Ref. 29 in the presence of 10 μCi of $^{45}CaCl_2$ and 2 μM $CaCl_2$ for 20 min at pH 7.5; nitrocellulose was then washed 3 times for 2 min with 10 ml of 30% ethanol. Radioactivity was detected with a Instant Imager, Packard.

The proteins were probed for the binding of $^{45}Ca^{2+}$ either in the presence or absence of DCCD (dissolved in ethanol). Control proteins were treated with the same volume of ethanol utilized for DCCD treatment (< 1.5% of the final volume) and incubated 10 min at room temperature. Calsequestrin from rabbit muscle was used as positive control.

All further procedures used plastic tubes to avoid contamination from other cations, and media made from deionized water (Elgastat Maxima, Elga Ltd., Bucks, United Kingdom; resistivity 18 MΩ), and passed through a Chelex 100 (Bio-Rad) column. Fresh stock solutions of Yb^{3+} were prepared just before use from chloride crystals ($YbCl_3 \cdot 6H_2O$, Aldrich) kept in a dessicator. The buffers used, *i.e.* HEPES, MES, and acetate, are known to be poor or weak lanthanide coordinators (25).

The reconstitution of Yb^{3+} into CP29 was performed on initial solutions of 1.85 mM CP29 in "Solution A" (0.03% dodecyl-β-maltoside (β-DM), 10 mM HEPES, pH 7.6, 0.1 M sucrose); all steps were performed at 4 °C in dim light. The CP29 protein solution was first diluted to 0.075 mM in 0.03% β-DM, 20 mM MES, 0.1 M sucrose, 1 mM EDTA all at pH 4.4. Similar pH conditions were found for the deionization procedure for the removal of Ca^{2+} and Mg^{2+} ions in bacteriorhodopsin (23). The resulting solution was then centrifuged in a Centricon 30 microconcentrator (Amicon) to remove the aqueous buffer. UV-visible absorption spectroscopy (Shimadzu UV-160) was used after every centrifugation step to verify no chlorophyll or carotenoid molecules were present in the wash. The CP29 protein was then re-diluted in a solution containing 0.03% β-DM, 0.1 M sucrose, 20 mM MES, pH 6.6, and 0.5 mM Yb^{3+}, representing a Yb^{3+}:CP29 ratio of approximately 10:1, and this solution was allowed to incubate overnight on ice in the dark. This Yb^{3+}-containing solution was then exchanged for the original Solution A by washing several times with Solution A using the Centricon 30 microconcentrators; again, UV-visible absorption spectrophotometry was used to verify no loss of protein or spectral changes in the native and Yb^{3+}-treated CP29. The Yb^{3+} content of the resulting CP29 protein, and after several consecutive washings in Solution A using the microconcentrators, was determined by graphite furnace atomic absorption spectrophotometry (Perkin-Elmer 2280) using the carefully determined linear relation observed for Yb^{3+} standard solutions.

Low temperature (15 K) near infrared Yb^{3+} vibronic side band spectra of Yb^{3+}-reconstituted CP29 were obtained as described in Roselli *et al*. (22, 23). Near-infrared light used for exciting the Yb^{3+} fluorescence was provided by a Ti^{4+}:sapphire laser (Spectra Physics 3900 S) pumped by a continuous wave Ar^+ laser (Coherent Innova 100) operating in the "all-lines" mode. Laser power at the sample was about 100 mW. Yb^{3+} near-infrared fluorescence was detected using a modified Bruker IFS 66 Fourier transform interferometer equipped with a Bruker FRA 100 Raman module as described by Roselli *et al*. (22, 23). Samples were held in an optical cold helium gas-flow cryostat (TBT-SMC, Grenoble, France). CP29 protein samples in D_2O were prepared by repeated cycles of solution exchanges with D_2O, 10 mM HEPES buffer, pD 8.0, containing 0.03% β-DM and 0.1 M sucrose using Centricon 30 concentrators; D_2O solutions are used as a precaution in Yb^{3+} VSB spectroscopy to avoid lanthanide fluorescence quenching often observed in H_2O (25). Spectral baseline correction, Fourier deconvolution, and second-derivative analyses were performed using the GRAMS 32 software package (Galactic Industries, Salem, NH).

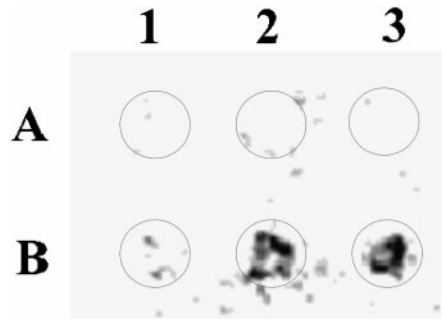

FIG. 1. **Effects of DCCD on calcium-binding properties of isolated LHCII and CP29.** Samples (after DCCD binding or treatment with the same volume of ethanol) were transferred on a nitrocellulose membrane with a dot blot apparatus. *A1* and *A2*, LHCII and CP29, respectively, incubated 10 min with 200 μM DCCD at room temperature; *B1* and *B2*, control LHCII and CP29 respectively; *A3*, blank; B3, calsequestrin.

RESULTS

$^{45}Ca^{2+}$ Binding in CP29 and LHCII—We have studied the binding of calcium to the minor antenna protein CP29 and to the major LHCII polypeptide. The dot blot analysis of purified CP29 and LHCII proteins (Fig. 1) demonstrates that CP29 is a calcium-binding polypeptide whereas LHCII did not show any significant binding (position B2 and B1, respectively, in Fig. 1). It should be pointed out that a weak signal is also present in the control LHCII protein, this signal was attributed to small contamination of minor antenna proteins (CP26 and CP29) in this preparation as confirmed by SDS-polyacrylamide gel electrophoresis analysis (not shown).

Fig. 1 also shows that DCCD prevented $^{45}Ca^{2+}$ binding to CP29 (position A2). This is in agreement with previous observations that radioactive calcium was specifically bound by unidentified PSII antenna proteins rather than by PSII core proteins and was displaced by DCCD (14).

One Persistent Yb^{3+} Ion Binding in CP29—Yb^{3+} can be reconstituted into CP29 by first lowering the pH to 4.4, washing, and then incubating CP29 in a 10-fold excess of Yb^{3+} in a buffered solution at pH 6.6. Excess Yb^{3+} ions, and those that were weakly bound, were removed by simple washing with Solution A with no chelator present. Fig. 2 shows the number of Yb^{3+} atoms per CP29, determined using graphite furnace atomic absorption spectrophotometry, as a function of the number of washing steps after Yb^{3+} reconstitution. This figure clearly shows that after only two washing steps, essentially all of the excess, and nonspecifically bound, Yb^{3+} is removed from CP29, resulting in the stoichiometric (1:1) binding of Yb^{3+} to the protein. These conditions for Yb^{3+} reconstitution procedure were determined after preliminary studies at higher pH.

Fluorescence of Yb^{3+} Reconstituted into CP29—Fig. 3 shows the Yb^{3+} fluorescence spectrum of the Yb^{3+}-reconstituted CP29 protein (Yb^{3+}-CP29) in the zero phonon line (or low frequency) region as compared with those of Yb^{3+} in the buffer/β-dodecyl maltoside D_2O solution (Yb^{3+}-β-DM) and Yb^{3+} in buffer/D_2O solution (Yb^{3+}-D_2O) (see legend in Fig. 3 for details). The fluorescence spectra in Fig. 3 are plotted in terms of absolute energy expressed in wavenumbers (cm^{-1}); the zero phonon lines are denoted "ZPL" and their absolute energies are indicated (10,236, 10,270, and 10,277 cm^{-1} for Yb^{3+}-CP29, Yb^{3+}-β-DM, and Yb^{3+}-D_2O, respectively). The vibronic side bands observed at lower energies are indicated as the shift (in

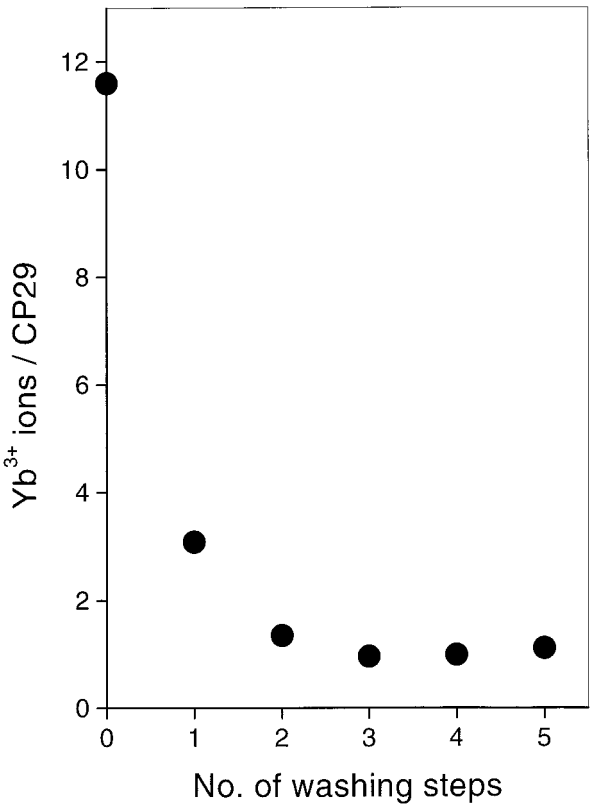

FIG. 2. **The amount of Yb^{3+} in CP29, determined by graphite furnace atomic absorption spectroscopy, as a function of the number of washing steps.**

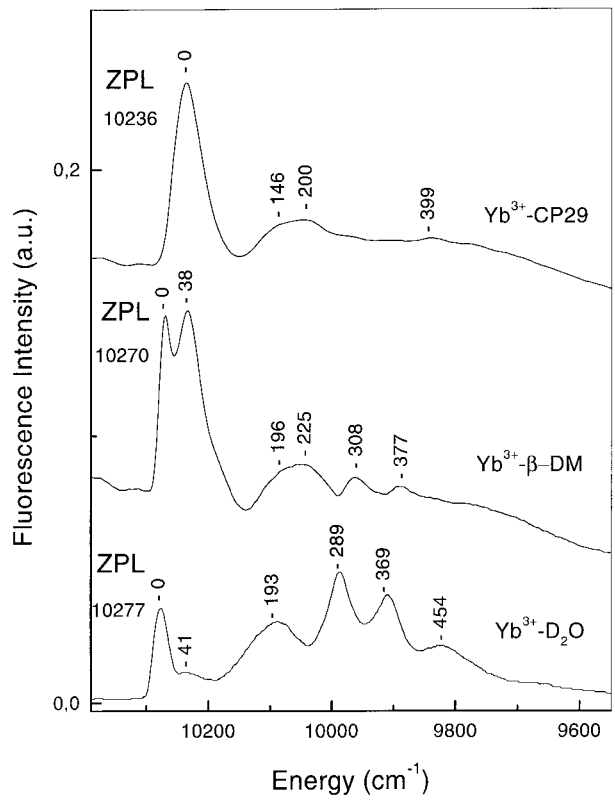

FIG. 3. **Low temperature (15 K) Yb^{3+} fluorescence spectra plotted in terms of absolute energy expressed in wave numbers (cm^{-1}) for Yb^{3+}-reconstituted CP29 protein in D_2O buffer (Yb-CP29, excited at 887.78 nm), Yb^{3+} complexed with 10-fold excess β-dodecylmaltoside in D_2O buffer (Yb-βDM, excited at 891.17 nm), and Yb^{3+} complexed with D_2O in D_2O buffer (Yb-D_2O, excited at 822.22 nm).** The energy of the ZPL are indictated in the figure (shown *horizontally*) and are expressed in absolute energy (cm^{-1}). The vibronic side band frequency values shown in the figure (shown *vertically*) are calculated from the shift in energy (cm^{-1}) from the ZPL. Spectra were shifted on the vertical scale for pictorial clarity.

cm^{-1}) relative to the ZPLs (0 cm^{-1}). Fig. 3 clearly shows that the Yb^{3+} VSB spectra of these different Yb^{3+} complexes (*i.e.* Yb^{3+}-CP29, Yb^{3+}-β-DM, and Yb^{3+}-buffer/D_2O) are all distinctly different. These different VSB spectra permit us to arrive at specific conclusions concerning the Yb^{3+}-CP29 complex. The VSB spectrum of Yb^{3+} complexed with D_2O is relatively strong and exhibits distinct characteristic VSB bands at 41, 193, 289, 369, and 454 cm^{-1} in the low frequency region. In comparing the low frequency VSB spectra of the Yb^{3+}-D_2O and Yb^{3+}-CP29 complex shown in Fig. 3 it is clear that the Yb^{3+} ion in CP29 is in a quite different coordination environment with few or no water molecules as ligands. In addition, comparison of the Yb^{3+}-CP29 and Yb^{3+}-β-DM low frequency VSB spectra indicates that we have no interference from possible Yb^{3+}-detergent complex artifacts in the Yb^{3+}-CP29 VSB spectrum (this point will be discussed further below).

The low frequency VSB spectrum of Yb^{3+}-reconstituted CP29 shown in Fig. 3 allows us to determine the ZPL of Yb^{3+} in CP29 along with some low-frequency ligand vibrational modes of the Yb^{3+} ligands, however, these low frequency modes are not as distinctive as higher frequency vibrational modes which serve as "vibrational fingerprints" of the ligands coordinated with Yb^{3+} in CP29. Fig. 4 shows the Yb^{3+} VSB spectra of Yb^{3+}-CP29, in the high frequency region, recorded using several excitation wavelengths. The VSBs are readily identified by their invariance in energy as the excitation wavelength is changed while, in contrast, Raman bands follow the change in excitation wavelength. Observed Raman bands in Fig. 4 are designated by "R"; with respect to the excitation wavelength, these clusters of Raman bands correspond to vibrational frequencies at about 2028–2414–2474 cm^{-1} (in Raman shift) and can be attributed to the D_2O ice in the samples. In contrast, there are three distinct bands in Fig. 4 at about 8900–8650 cm^{-1} (on the absolute energy scale) that do not shift as the excitation wavelength is changed and can be thus confidently assigned to vibronic side bands of the Yb^{3+} in CP29. These three distinct VSB bands in Fig. 4 are seen at 1,314, 1,397, and 1,597 cm^{-1}, as calculated from the shift of the ZPL of the Yb^{3+}-CP29 complex observed at 10,236 cm^{-1} (Fig. 3). We also note that these VSBs are unique to the Yb^{3+}-CP29 complex and are not observed for the Yb^{3+}·β-dodecylmaltoside complex (Fig. 4) nor for the Yb^{3+}·D_2O complex (data not shown). Furthermore, at these wavelengths of excitation we could not detect any interference from any Raman contributions from either the protein or its chlorophyll/carotenoid pigments in the VSB spectral region studied.

As with any fluorescence phenomena, the intensity of the fluorescence band is excitation wavelength dependent. We have analyzed the behavior of the VSB bands as a function of excitation energy. Fig. 5 shows the variation in intensity of the ZPL, two low frequency VSBs, as well as the relatively intense 1397 and 1597 cm^{-1} VSBs, in the high frequency region, of Yb^{3+} in CP29, as a function of excitation wavelength. The intense, sharp 2028 cm^{-1} Raman band of the D_2O ice (denoted *R* in Fig. 4) was used as an internal intensity standard. As expected, the intensities of the two VSBs vary as the excitation wavelength is changed but more importantly, the trends of the VSBs are all the same. In addition, in the low frequency region, the 399 cm^{-1} VSB and the two unresolved 146 and 200 cm^{-1} VSBs follow the same trend as the ZPL; for these two latter bands, the intensity was monitored near the center frequency

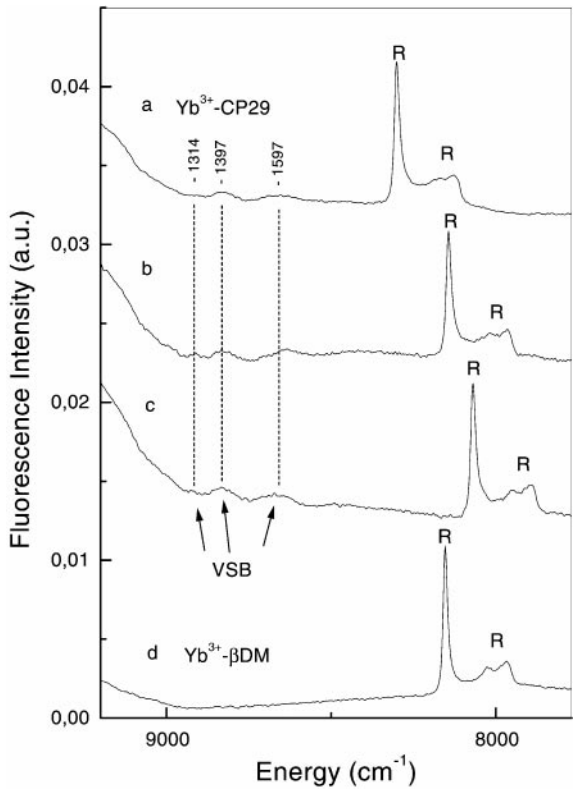

FIG. 4. **Low temperature (15 K) fluorescence spectra of Yb^{3+} in Yb^{3+}-CP29 excited at 943.75 nm (*a*), 957.85 nm (*b*), 964.79 nm (*c*), and fluorescence (*d*) of Yb^{3+} in Yb^{3+}-β-dodecylmaltoside complex excited at 957.67 nm.** The bands marked with "*R*" to designate Raman bands of D_2O ice are seen to shift on the absolute energy scale (cm^{-1}) as the excitation wavelength is changed. The Yb^{3+} VSB do not shift as the excitation wavelength changes, and prominent VSBs are observed in Yb^{3+}-CP29 at 1,314, 1,433, and 1,597 cm^{-1} (indicated *vertically* in the figure) as calculated from the shift with respect to the ZPL at 10,236 cm^{-1} (see Fig. 2). These latter VSBs are unique for Yb^{3+} in CP29 and are not observed in the Yb^{3+}-β-dodecylmaltoside complex (*d*). Spectra were shifted on the vertical scale for pictorial clarity.

of 170 cm^{-1}. In the high frequency region,[2] the 1397 and 1597 cm^{-1} VSBs exhibit similar trends as the wavelength of excitation is changed and indicate the same maximum at about 960 nm. If these two VSB bands were originating from two or more spectroscopically different Yb^{3+} sites, then it is expected that their excitation wavelength-dependent behavior would be different and would manifest this difference by variation in the trends of the VSB bands. The Yb^{3+} VSB technique is very sensitive to this type of behavior, as we have previously reported (23, 30). The lack of differences in the observed VSB intensities as a function of excitation wavelength as seen in Fig. 5 indicates that the population of Yb^{3+} ions detected in CP29 protein is spectroscopically homogenous. We note that Yb^{3+} VSB spectroscopy is a very sensitive technique and can distinguish energy differences in Yb^{3+}-binding sites as small as 15 cm^{-1} (30).

Fig. 6 shows the unsmoothed average of eight high frequency VSB spectra of Yb^{3+} in CP29. For clarity of presentation, a baseline correction has been performed. In addition to the prominent VSBs observed at 1314, 1397, and 1597 cm^{-1}, we have performed Fourier deconvolution and second-derivative analyses (not shown) to accurately determine the frequencies of unresolved shoulders seen at 1433, 1533, and 1623 cm^{-1} in the VSB spectrum. We note that the comparison of the Fourier deconvolution and second-derivative spectra were both in agreement in identifying spectral components at 1433, 1533, and 1623 cm^{-1}. The Yb^{3+} VSB spectrum shown in Fig. 6 is similar to that of Yb^{3+} reconstituted into the Ca^{2+}-binding site of rabbit muscle parvalbumin (22) and of other complexes of Yb^{3+} predominantly bound by carboxylic groups (22, 23, 30). The VSB spectrum in Fig. 6 unambiguously indicates that the majority of the ligands of Yb^{3+} bound in CP29 are carboxylic acids, as would be expected for a Ca^{2+}-binding site. Details of the spectrum and band assignments will be discussed below.

[2] For technical reasons related to the spectral characteristics of the laser-rejection filters used in our apparatus, we are unable to observe the ZPL line when measuring the high frequency VSBs. Consequently, the VSB data are depicted separately in the low frequency and the high frequency VSB spectral ranges.

DISCUSSION

Lanthanide (Yb^{3+}) Reconstitution into Protein Ca^{2+}-binding Sites—It is well established that lanthanides readily substitute and strongly bind in protein Ca^{2+}-binding sites (22–25, 30, 31). Trivalent lanthanides have ionic radii (32) which are comparable to that of Ca^{2+} (about 1 Å). Like Ca^{2+}, lanthanide bonding is essentially ionic (25). Crystallographic, spectroscopic, and chemical data indicate that the most common ligand atoms of Ca^{2+}-binding sites in biological systems are oxygen atoms (33–35). Similarly, lanthanides exhibit a strong preference for ligands providing oxygen donor atoms (25). Lanthanides have been used extensively to probe Ca^{2+}-binding sites in proteins (reviewed in Refs. 25, 31, and 36) and x-ray crystallographic protein structures provide strong evidence for the isomorphous replacement of Ca^{2+} by trivalent lanthanides (25, 36). Several structures suggest that it is quite generally possible to replace Ca^{2+} by Ln^{3+} with minimal disruption to the binding site or the overall structure of the protein. It should be expected, however, that the Ca^{2+} to Ln^{3+} substitution could increase the co-ordination number by one (36), as has been observed in one Ca^{2+} site of carp parvalbumin which was substituted with Yb^{3+} (37).

Concerning the activity of the Ln^{3+}-substituted proteins, there are examples cited in the literature where retention of full biological activity, diminished activity, and inhibitory behavior are reported. The first case will likely result in situations where the Ln^{3+} like the Ca^{3+} play a purely structural role. If Ca^{2+} is present at a catalytic site, then some change in activity is to be expected (36).

Although the comparable ionic radii and co-ordination chemistries of Ca^{2+} and the Ln^{3+} ions render near-perfect structural replacements, the decreased lability toward ligand exchange and stronger binding of the lanthanides must be considered when using these ions as probes. Although they are not perfect analogues of Ca^{2+} in all functional respects, their spectroscopic properties render them extremely valuable in probing spectroscopically silent Ca^{2+}-binding sites. (36).

The Ca^{2+}- and Yb^{3+}-binding Sites in CP29—In this work we have identified and confirmed CP29, the 29-kDa chlorophyll *a*/*b*-binding protein associated with Photosystem II, as a Ca^{2+}-binding protein (Fig. 1). Treatment of CP29 at pH 4.4 and reconstitution with Yb^{3+} results in the 1:1 stoichiometric binding of Yb^{3+} ion in CP29 as determined by graphite furnace atomic absorption spectrophotometry (Fig. 2). Lanthanides can be replaced for Ca^{2+} in Ca^{2+}-binding proteins either by placing the native or the apoprotein in contact with the lanthanide solution (25). The method we have used (see "Experimental Procedures") was developed for the reconstitution of Yb^{3+} into a fragile, temperature- and light-sensitive, detergent-solubilized protein of limited quantity. The treatment of CP29 at pH 4.4 before significant incorporation of Yb^{3+} into the protein metal-binding site was observed is consistent with the weakened binding or release of Ca^{2+} from carboxyl group ligands (25) to facilitate metal exchange with Yb^{3+}. In addition, the

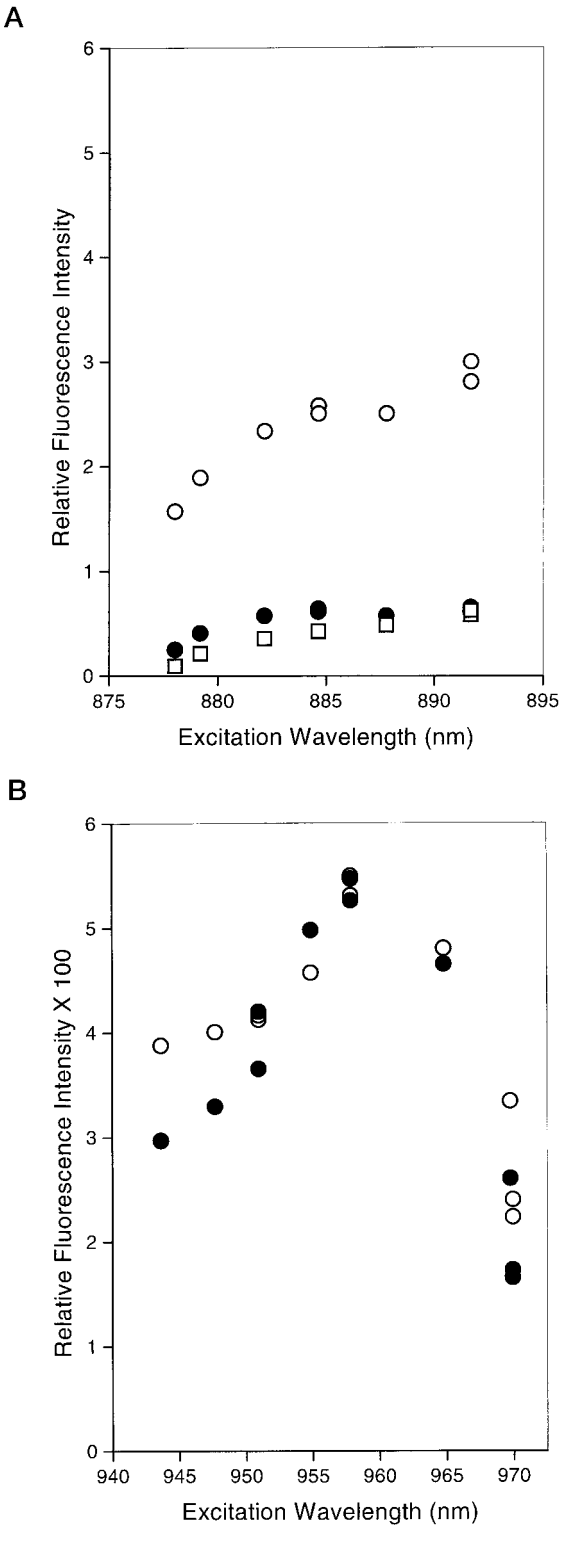

FIG. 5. **Variation of the intensities of: (*A*) the ZPL (○) and the low frequency 170 (□) and 399 (●) cm^{-1}, and (*B*) the high frequency 1397 (○) and 1597 (●) cm^{-1} vibronic side bands of Yb^{3+} in CP29 as a function of excitation wavelength.** The intensities were normalized to the 2028 cm^{-1} Raman band of D_2O which was used as an internal standard. The data for the 170 cm^{-1} (□) VSB is taken as the central frequency of the unresolved VSBs at 146 and 200 cm^{-1} (see Fig. 3).

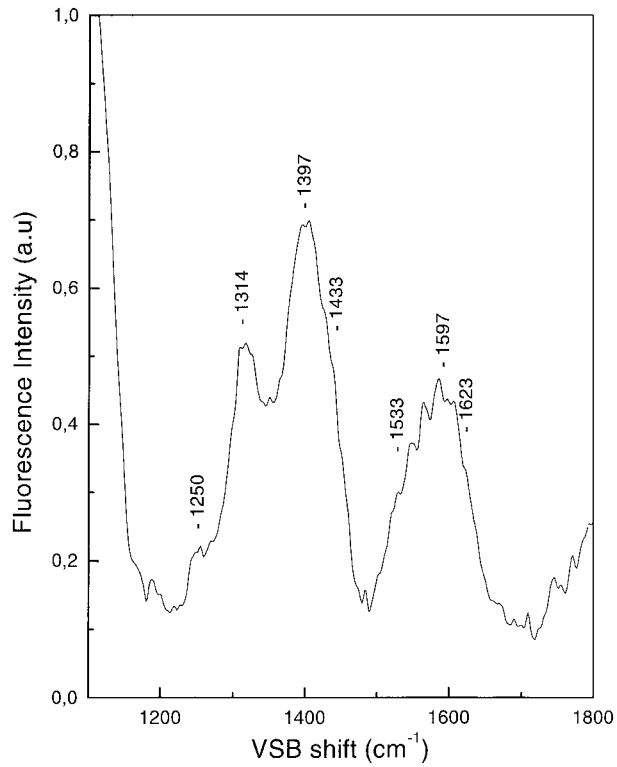

FIG. 6. **Low temperature (15 K) high frequency vibronic side band spectrum of Yb^{3+} reconstituted into CP29.** This spectrum represents an average of 8 individual VSB spectra recorded at various wavelengths. For clarity, a baseline has been subtracted. Spectral components designated at 1433, 1533, and 1623 cm^{-1} were obtained by Fourier transform deconvolution and second-derivative analyses.

lack of observed changes in relative intensities of the Yb^{3+} fluorescence vibronic side bands as excitation wavelength was changed indicates that the Yb^{3+} site being probed is originating from one site or one species. All these data indicate that the Yb^{3+} ion which has been reconstituted into CP29 is strongly and specifically bound in a well defined metal-binding site. The above behavior is consistent with Yb^{3+} replacing Ca^{2+} in the metal-binding site of CP29.

It should be mentioned that in many studies on Ca^{2+} removal from the intact PSII complex, only the Ca^{2+} involved in oxygen evolution, and thus the Ca^{2+} most closely associated with the PSII reaction center core, was reported to be removed (reviewed in Ref. 1; see also Ref. 6) whereas the other Ca^{2+} ion associated with the extrinsic polypeptides remained. Some treatments, such as that described by Ono and Inoue (38), descend in pH values lower (*i.e.* pH 3) than that used in the Ca^{2+} deionization step for CP29 in our work. However, in those studies the treatments were performed on intact PSII membrane fragments and not on the isolated single polypeptide as is the case in our work here where the replacement of Ca^{2+} in CP29 by Yb^{3+} may have been greatly facilitated due to the fact that the protein is in an isolated detergent-solubilized form rendering the Ca^{2+}-binding site more susceptible to ion exchange.

The ligands of Yb^{3+}/Ca^{2+} in CP29—Based on its similarity with the Yb^{3+} vibronic side band spectra of Yb^{3+}-carboxylic ligand complexes and with Yb^{3+}-reconstituted Ca^{2+}-binding proteins with carboxylic ligands (see Fig. 2 in Ref. 22), the VSB spectrum of Yb^{3+} bound in CP29 clearly indicates a majority of carboxylic acid ligands. This is what would be expected for a Ca^{2+}-binding site. Indeed lanthanides and calcium are known to have a strong affinity for oxygen ligands (25). Previously, we have systematically studied the infrared absorption and the fluorescence VSB spectra of many various Yb^{3+} model complexes, several of which contain carboxylate groups (COO^-), carbonyl groups (C=O), as well as alcohol and phenolic C-O groups (22, 23, 30). VSB assignments of these groups could

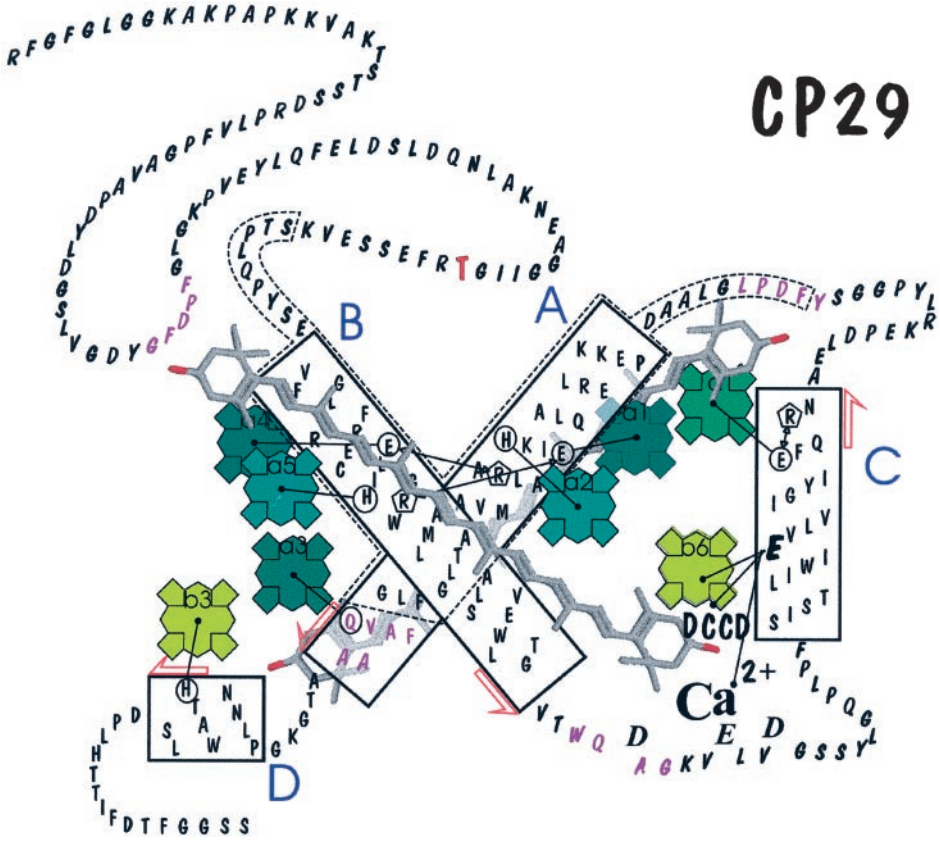

FIG. 7. **Model for the location of the calcium-binding site in CP29.** The residue involved in the binding of DCCD (Glu-166) is located in an hydrophobic region of helix C. Three acidic residues are present in the lumenal loop and they could be directly involved in calcium binding.

easily be made based on the well known characteristic vibrational frequencies (or fingerprints) of these groups. This approach was successfully applied to the case of well known Ca^{2+}-binding proteins, such a rabbit muscle parvalbumin whose Ca^{2+}-binding sites are rich in COO^- ligands, and include protein backbone C=O groups as well as C-O groups from alcoholic side chains such as serine (22).

Like calcium, lanthanides can bind carboxylic acids in a monodentate or bidentate manner. The symmetric, ν_{sym}, and antisymmetric, $\nu_{antisym}$, vibrational stretching modes of COO^- are expected at about 1400–1450 cm^{-1} and about 1550–1600 cm^{-1}, respectively (22, 23, 39). For monodentate coordination, the difference, $\Delta\nu$, in these two vibrational modes is about 200 cm^{-1} while for bidentate coordination $\Delta\nu$ is about 100 cm^{-1} (39). In the VSB spectrum of Yb^{3+}, the most intense bands are observed at 1397 and 1597 cm^{-1}; these bands are assignable as the symmetric ν_s and antisymmetric $\nu_{antisym}$ vibrational modes of the COO^- ligands of Yb^{3+}. The difference in vibrational frequency, $\Delta\nu$, of these two modes is 200 cm^{-1} indicating COO^- ligands of monodentate coordination. This indicates that most of the COO^- ligands are coordinated to Yb^{3+} in a monodentate manner. However, we cannot conclude that all of the COO^- ligands are monodentate. The 1397 and 1597 cm^{-1} bands are broad (about 100 cm^{-1} full width at half-maximum), asymmetric, and clearly indicate the presence of unresolved shoulders. Two shoulders, whose vibrational frequencies have been determined by Fourier deconvolution and second-derivative analyses to be 1433 and 1533 cm^{-1} can also be assigned to ν_{sym} and $\nu_{antisym}$ modes, respectively. For this case, the difference in frequency, $\Delta\nu$, is 100 cm^{-1} and thus indicates bidentate binding of the COO^- group(s) giving rise to the 1433 and 1533 cm^{-1} VSBs. It is difficult to accurately quantify the number of monodentate and bidentate COO^- ligands to Yb^{3+} in CP29, but considering the intensities of the 1397/1597 cm^{-1} VSBs relative to the intensities of the weaker 1433/1533 cm^{-1} VSBs, the

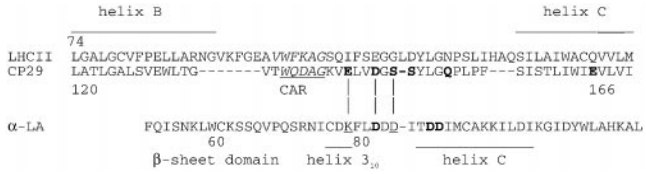

FIG. 8. **Partial amino acid sequences of CP29 in the lumenal loop region between the purported transmembrane α-helices B and C aligned with that of LHCII (Ref. 26), and compared with the Ca^{2+}-binding site of α-lactalbumin, α-LA (Ref. 42).** The residues which coordinate the Ca^{2+} in α-lactalbumin are indicated in *boldface* (three aspartic acid residues binding via their carboxyl groups) and *underlined* (residues binding via their backbone carbonyl groups). The CP29 residues shown in *boldface* indicate possible Ca^{2+}-binding residues, possessing COO^- or OH^- groups; the *underlined* residues in *italics* *WQDAG* are part of the carotenoid binding pocket.

bidentate COO^- ligands are a minority, perhaps representing only one bidentate COO^- ligand to three or four monodentate COO^- ligands.

The 1623 cm^{-1} VSB component we have identified using Fourier deconvolution and second-derivative analyses on the VSB spectrum in Fig. 6 is assignable to the vibrational stretching frequency of a carbonyl C=O group coordinated to Yb^{3+} (Table I in Ref. 22, and references therein). Carbonyl (C=O) groups are also good Ca^{2+} and Yb^{3+} ligands. These C=O groups are expected to vibrate at about 1620 cm^{-1}, based on the infrared and Yb^{3+} VSB spectra of Yb^{3+} complexes with ligands possessing such groups (22). Because of their similar vibrational frequencies, the C=O bands (about 1620 cm^{-1}) and the monodentate COO^- $\nu_{antisym}$ modes (about 1600 cm^{-1}) are often difficult to resolve. The VSB spectrum of Yb^{3+} in CP29 indicates that at least one C=O group, most likely from the protein backbone, is a ligand.

The 1314 cm^{-1} VSB in Fig. 6 is assignable to a C-O group (22). This value is slightly too high to arise from a phenolic C-O

group which would be expected at about 1270–1280 cm^{-1} such as that from a tyrosine residue (23), but is more consistent with a C-O group from an alcoholic side chain, such as serine.

Based on the above analysis we can deduce the following ligands for Yb^{3+} reconstituted in CP29: a majority of monodentate COO^- groups and at least one bidentate COO^- group from carboxylic acid residue side chains, at least one C=O group from the protein backbone, and at least one C-O group from an alcoholic side chain. In the absence of an intense VSB at about 2700 cm^{-1}, we find no evidence for the presence of D_2O as a ligand of Yb^{3+} reconstituted into CP29.

Location of the Yb^{3+}-/Ca^{2+}-binding Site in CP29—CP29 is homologous to the major light harvesting complex of Photosystem II (LHCII) whose structure has been recently determined (40). Accordingly, three transmembrane hydrophobic helices (A-C) and a lumenal surface amphiphilic helix (D) can be identified connected by two helix-helix loops on either side of the membrane, a stromal exposed N-terminal extension and a lumen exposed C terminus. According to the availability of clustered acidic residues, two domains are eligible for Yb^{3+}-/Ca^{2+}-binding: the N terminus, protruding into the stromal space, and the lumen exposed domain including part of helix C and the loop extending to helix B. A structural model of the CP29 protein has been recently proposed (41).

In order to probe the two possible locations for the Ca^{2+}-binding site, we have treated the protein with DCCD, a protein modifying agent reacting with acidic residues in hydrophobic environments, such as those within α-helices. In the case of CP29, DCCD has been shown to bind to a glutamic acid residue (Glu-166) in helix C (26) (see Fig. 7) which is part of the lumen-exposed putative Ca^{2+} binding sequence. In the case Glu-166 is involved in binding Ca^{2+} or is near the Ca^{2+}-binding site, we would expect that DCCD treatment would prevent Ca^{2+} binding.

Fig. 1 showed that DCCD prevented $^{45}Ca^{2+}$ binding to CP29 (position A2) thus confirming that Glu-166 is part of, or near to, the Ca^{2+}-binding site. Within our structural model, Glu-166 is found in helix C and is the only acidic residue in CP29 that is in a hydrophobic environment and is not charge compensated by neighboring arginine residues. On the basis of competition with DCCD for the Glu-166 residue (26), the region involved in Ca^{2+} binding can be located in the domain including the lumenal loop between helices B and C, and, perhaps, part of the hydrophobic helix C. In this region, three acidic residues are present (2 Asp and 1 Glu) that could be part of the binding site. A structural model for CP29 (41) and its putative Ca^{2+}-binding site is shown in Fig. 7.

The helix-loop-helix EF-hand is by far the most common motif recognized for intracellular Ca^{2+}-binding proteins (35). In the so-called EF-hand motif, the Ca^{2+} ion is bound in a loop consisting of 10–14 amino acids forming a tight turn between two helices. The proposed Ca^{2+}-binding domain in the CP29 structural model of Fig. 7 is the loop between helices B and C. This loop is not recognized as typical of a regular EF-hand because it is too long (*i.e.* more than 12 amino acid residues). Interestingly, we have noted significant homology in the partial sequence alignment of the purported Ca^{2+}-binding domain of the polypeptide CP29 and that of the Ca^{2+}-binding protein(s) α-lactalbumin (see Fig. 8). As in an EF-motif, the Ca^{2+}-binding site in α-lactalbumin is also formed by two helices and a loop joining them but compared with the EF-hand, the loop is shorter by about 2 amino acid residues and the arrangement of the structural units are different (42). However, this helix-loop-helix "elbow" motif in α-lactalbumin would not be consistent with the structural model of CP29 in Fig. 7 which shows a relatively large loop domain between helices B and C. Thus, the Ca^{2+}-binding site domain of CP29 identified in this work may be regarded as having a structural motif atypical or uncommon as compared with the known binding motifs of most Ca^{2+}-binding proteins. The unusual character of the Ca^{2+}-binding site in CP29 may be related to the Ca^{2+} ion's proximity to chlorophyll and carotenoid molecules and/or to a specific function or role of the Ca^{2+} ion.

It is surprising that CP29 is the only Ca^{2+}-binding antenna protein since it belongs to a protein family which includes at least 10 members, six of which, Lhca1–4, Lhcb4–5, carry a glutamate residue in positions homologous to Glu-166 in CP29. However, sequence comparison in this region shows that CP29, with respect to other Lhc gene products, is unique in carrying not only the glutamic residue in position 166, but also the three acidic residues in the loop. Site-directed mutagenesis work has recently shown that Glu-166 is also involved in the binding of chlorophyll as well as in carotenoid (violaxanthin) binding (41).

It is interesting to observe that the glutamic acid residues involved in chlorophyll coordination in LHCII (40) were found to be charge-compensated by arginine residues. However, in the case of CP29, no basic residue can be found in positions compatible with Glu-166 charge compensation. We can therefore hypothesize that the Ca^{2+} ion may perform the role of the arginine in compensating the charge on the glutamate, thus allowing it to act as a ligand to the chlorophyll. It was proposed (43) that photoprotective dissipation of excess energy in the PSII antenna, elicited by low lumenal pH, is triggered by protonation of an acidic residue in a hydrophobic environment thus leading to a structural change involving a closer association between the chlorophyll and a carotenoid molecule. Within this model, Ca^{2+} coordination to the acidic residues making up the coordination sphere of the Ca^{2+} could be involved in such a pH triggered structural change.

Acknowledgments—We thank Dr. Alessandra Nori (University of Padua) for advice in Ca^{2+} overlay procedures and for the kind gift of purified calsequestrin. Roberta Croce is thanked for help in the purification of CP29 and helpful discussion. Dr. Alain Boussac (CEA/Saclay) is thanked for helpful discussions.

REFERENCES

1. Debus, R. J. (1992) *Biochim. Biophys. Acta* **1102,** 269–352
2. Rutherford, A. W., Zimmermann, J.-L., and Boussac, A. (1992) in *The Photosystems: Structure, Function, and Molecular Biology* (Barber, J., ed) pp. 179–229, Elsevier
3. Britt, R. D. (1996) in *Oxygenic Photosynthesis: The Light Reactions* (Ort, D. R., and Yocum, C. F., eds) pp. 137–164, Kluwer Academic, The Netherlands
4. Yocum, C. F. (1991) *Biochim. Biophys. Acta* **1059,** 1–15
5. Han, K.-C., and Katoh, S. (1993) *Plant Cell Physiol.* **34,** 585–593
6. Ädelroth, P., Lindberg, K., and Andréasson, L.-E. (1995) *Biochemistry* **34,** 9021–9027
7. Krieger, A., and Weiss, E. (1993) *Photosynth. Res.* **37,** 117–130
8. Chen, C., and Cheniae, G. (1995) in *Photosynthesis: from Light to Energy* (Mathis, P., ed) Vol. II, pp. 329–332, Kluwer Academic Press, Dordrecht
9. Chu, H. A., Nguyen, A. P., and Debus, R. J. (1995) *Biochemistry* **34,** 5839–5858
10. Qian, M;, Dao, L., Debus, R. J., and Burnap, R. L. (1999) *Biochemistry* **38,** 6070–6081
11. Shen, J.-R., Satoh, K., and Katoh, S. (1988) *Biochim. Biophys. Acta* **936,** 386–394
12. Irrgang K.-D, Renger, G., and Vater, J. (1991) *Eur. J. Biochem.* **201,** 515–522
13. Davis, D. J., and Gross, E. L. (1975) *Biochim. Biophys. Acta* **387,** 557–567
14. Webber, A. N., and Gray, J. C. (1989) *FEBS Lett.* **249,** 79–82
15. Jansson, S. (1994) *Biochim. Biophys. Acta* **1184,** 1–19
16. Bassi, R., Pineau, B., Dainese, P., and Marquardt, J. (1993) *Eur. J. Biochem.* **212,** 297–303
17. Giuffra, E., Zuchelli, G., Sandonà, D., Croce, R., Cugini, D., Garlaschi, F. M., Bassi, R., and Jennings, R. C. (1997) *Biochemistry* **36,** 12984–12993
18. Sandonà, D., Croce, R., Pagano, A., Crimi, M., and Bassi, R. (1998) *Biochim. Biophys. Acta* **1365,** 207–214
19. Walters, R. G., Ruban A. V., and Horton, P. (1994) *Eur. J. Biochem.* **226,** 1063–1069
20. Croce, R., Breton, J., and Bassi, R. (1996) *Biochemistry* **35,** 11142–11148
21. Bergantino, E., Dainese, P., Cerovic, Z., Sechi, S., and Bassi, R. (1995) *J. Biol. Chem.* **270,** 8474–8481
22. Roselli, C., Boussac, A., and Mattioli, T. A. (1994) *Proc. Natl. Acad. Sci. U. S. A.* **91,** 12897–12901
23. Roselli, C., Boussac, A., Mattioli, T. A., Griffiths, J. A., and El-Sayed, M. (1996) *Proc. Natl. Acad. Sci. U. S. A.* **93,** 14333–14337
24. Horrocks, W. de W., Jr. (1982) *Adv. Inorg. Biochem.* **4,** 201–261

25. Evans, C. H. (1990) in *Biochemistry of the Lanthanides* (Freiden, E., ed) Plenum Press, New York
26. Pesaresi, P., Sandonà, D., Giuffra, E., and Bassi, R. (1997) *FEBS Lett.* **402,** 151–156
27. Dainese, P., Hoyer-Hansen, G., and Bassi, R. (1990) *Photochem. Photobiol.* **51,** 693
28. Dainese, P., and Bassi, R. (1991) *J. Biol. Chem.* **266,** 8136–8142
29. Maruyama, K., Mikawa, T., and Ebashi, S. (1984) *J. Biochem.* **95,** 511–519
30. Roselli, C., Burie, J.-R., Mattioli, T. A., and Boussac, A. (1995) *Biospectroscopy* **1,** 329–339
31. Martin, R. B., and Richardson, F. S. (1979) *Q. Rev. Biophys.* **12,** 181–209
32. Shannon, R. D. (1976) *Acta Crystallogr. Sect. A* **32,** 751–767
33. Einspahr, H., and Bugg, C. E. (1984) in *Metals in Biological Systems* (Sigel, H., ed) Vol. 17, pp. 51–97, Marcel Dekker, New York
34. MacPhalen, C. A., Strynadka, N. C. J., and James, M. N. G. (1991) *Adv. Protein Chem.* **42,** 77–144
35. Finn, B. Y., and Drakenberg, T. (1999) *Adv. Inorg. Chem.* **46,** 441–494
36. Horrocks, W., de W., Jr. (1993) *Methods Enzymology* **226,** 495–538
37. Kumar, V. D., Lee, L., and Edwards, B. F. P. (1991) *FEBS Lett.* **283,** 311–316
38. Ono, T., and Inoue, Y. (1988) *FEBS Lett.* **227,** 147–152
39. Nakamoto, K. (1963) *Infrared of Inorganic and Coordination Compounds*, Wiley, New York
40. Kühlbrandt, W., Wang, D. N., and Fujiyoshi, Y. (1994) *Nature* **367,** 614–621
41. Bassi, R., Croce, R., Cugini, D., and Sandonà, D. (1999) *Proc. Natl. Acad. Sci. U. S. A.* **96,** 10056–10061
42. Acharya, K. R., Stuart, D. L., Walker, N. P. C., and Phillips, D. C. (1989) *J. Mol. Biol.* **208,** 99–127
43. Crofts, A. R., and Yerkes, C. T. (1994) *FEBS Lett.* **352,** 265–270

Calcium Binding to the Photosystem II Subunit CP29

Caroline Jegerschöld, A. William Rutherford, Tony A. Mattioli, Massimo Crimi and Roberto Bassi

J. Biol. Chem. 2000, 275:12781-12788.
doi: 10.1074/jbc.275.17.12781
